Available online at www.sciencedirect.com
SCIENCE DIRECT®
Computational Materials Science 36 (2006) 84–90
COMPUTATIONAL MATERIALS SCIENCE
www.elsevier.com/locate/commatsci

Dilute magnetic III–V semiconductor spintronics materials: A first-principles approach

G.P. Das [a,*], B.K. Rao [b,✠], P. Jena [b], Y. Kawazoe [c]

[a] Department of Materials Science, Indian Association for the Cultivation of Science, Jadavpur, Kolkata 700032, India
[b] Department of Physics, Virginia Commonwealth University, Richmond, VA 23284, USA
[c] Institute for Materials Research, Tohoku University, Sendai 980-8577, Japan

Abstract

Group-III nitride semiconductors, such as GaN, when doped with 3d transition metals such as Mn or Cr show ferromagnetism with high Curie temperature. Such dilute magnetic semiconductors (DMS) with larger band gaps and smaller lattice constants compared to GaAs based DMS, are potential candidates for room temperature spintronics devices. We have investigated the magnetic coupling between doped Mn (or Cr) atoms in clusters as well as crystals of GaN from first principles using molecular orbital theory for $(GaN)_xTM_2$ clusters and TB-LMTO band calculations for wurtzite structured $(Ga_{14}TM_2)N_{16}$ supercells. Our calculations reveal that the coupling between TM-impurity atoms is ferromagnetic with a bulk magnetic moment of $\sim$3.5 μ_B per Mn atom and $\sim$2.7 μ_B per Cr atom.

Keywords: Dilute magnetic semiconductors; Spintronics; First-principles calculations; Cluster calculations; LMTO supercell

1. Introduction

The information revolution that we are experiencing today puts increasing demand for faster, smaller, low power and high storage capacity devices for processing of information. Current state of the art semiconductor devices have already come to the stage where it is approaching the fundamental limit of miniaturization, e.g., the width of gate electrodes in a Si-based microprocessor has reduced to $\leqslant$1.5 nm where quantum effects become predominant. Question is what next? Scientists, especially device physicists are looking for radically new pastures such as molecular electronics, magneto-electronics, spin electronics and polymer electronics. "Spintronics" is the short form of spin-based electronics where one exploits electron's spin, over and above its charge, in order to carry information. This new discipline exploits the inherent quantum properties of electrons for various kinds of logic, storage and sensor applications via spin-polarization, spin-injection, spin-transport, spin-coherence, spin-tracing, spin-valve etc. [1]. The first successful example of spintronics is the giant magneto-resistance (GMR) effect in Fe/Cr metallic multilayers [2]. GMR is defined as the relative change in conductivity between parallel and anti-parallel spin configurations of the ferromagnetic layers. This effect arises due to confinement of electrons in quantum wells formed in the nonmagnetic layer by the spin-dependent potentials of the ferromagnetic layers [3]. Semiconductor spintronics is a relatively new field that started in the late 90s when it was shown that nonmagnetic III–V semiconductors (such as GaAs) can be made ferromagnetic via doping of transition metal atoms (such as Mn) and the Curie temperature T_c was found to be

* Corresponding author. Tel.: +91 33 24734971; fax: +91 33 24732805.
E-mail address: msgpd@iacs.res.in (G.P. Das).
✠ Deceased.

0927-0256/$ - see front matter © 2005 Elsevier B.V. All rights reserved.
doi:10.1016/j.commatsci.2005.07.004

≈110 K [4]. The explanation was given by Dietl et al. [5] in terms of exchange coupling between the localized spins of d^5 configuration Mn with the delocalized (or weakly localized) holes residing in a p-like valence band, and the same argument was used to estimate T_c's for other III–V and II–VI semiconductors doped with 5% Mn. It was predicted that T_c can be pushed above room temperature when some 3d TM is doped into GaN or ZnO which are two most extensively studied wide band-gap semiconductors because of their applications in blue lasers and optoelectronic devices [6]. Following this prediction of achieving ferromagnetism in GaN, there was an avalanche of experimental works on the (GaMn)N system, which however resulted in more controversies than consensus. While some groups have reported antiferromagnetic behavior, others have observed ferromagnetism with various different values of T_c ranging from 20 K to 940 K [7]. Most of these results are on thin film samples for which substrate conditions play a crucial role. In the flurry of experimental attempts to synthesize ferromagnetic semiconductors with T_c close to room temperature, Cr doped GaN has also been recently grown successfully in the form of bulk single crystal using a sodium flux grown method, and the T_c is observed to be around 280 K [8].

2. Ferromagnetism in GaN DMS

This discovery of high T_c ferromagnetism in Mn (Cr)-doped GaN samples have given rise to several important observations.

(a) Cr and Mn are both antiferromagnetic in bulk phase and when doped into GaN, these impurity atoms go to Ga-substitutional site as Cr^{3+} and Mn^{3+} valence state in d^3 and d^4 configurations respectively. This indicates that a magnetic impurity such as Mn or Cr contributes spins as well as holes (p-type doping) to the III–V semiconductors such as GaN.

(b) The origin of ferromagnetism in Mn doped III–V semiconductors was first explained by Dietl et al. [5] in terms of carrier-mediated RKKY interaction or Zener model, in which antiferromagnetic (AFM) exchange coupling partially spin polarizes the holes present in the system, which in turn causes an alignment of the local Mn spins. This model, however, assumes high hole density $\sim 10^{20}$ and the existence of Fermi surface.

(c) Later, Litvinov and Dugaev [9] used a model based on virtual acceptor level to valence band transitions, and provided a detailed quantitative prediction of the dependence of the Curie temperature on the Mn concentration for various wurtzite III–V alloys.

(d) Using local density supercell band calculations for 3d transition metal (TM) doped III–V zinc-blende semiconductors, van Schilfgaarde and Mryasov [10] had shown that the anomalous exchange interactions between the impurity atoms deviate strongly from the RKKY-like simple models and undergo a transition from ferromagnetic (for Mn and Cr) to antiferromagnetic (for Fe) as a function of d-band filling.

(e) Sato and Katayama-Yoshida [11], had carried out KKR-CPA calculations in randomly substituted 3d TM impurities in GaN and found ferromagnetic state to be stable for half-filled or less than half-filled impurities such as V, Cr, and Mn, while a spin-glass like state is found to be stable for more than half-filled impurities Fe, Co, and Ni.

The investigations by these latter two groups [10,11] independently confirm the experimental observations of Mn and Cr atoms coupling ferromagnetically in GaN. For further details, the reader may refer to some of the recent theoretical works reported in this field [12].

3. First principles calculations

We have carried out first principles investigation of TM_2 dimer (TM = Mn and Cr) doped GaN in various structural forms that simulate binding of TM onto surface as well as bulk sites [13,14]. The reason why we have used TM_2-dimer rather than a single TM impurity atom is that we are interested to see the strength of magnetic coupling and compare it with our cluster results. All the results reported in this work are based on density functional theory with gradient corrected exchange-correlation functional. The details of the methodologies used, both for cluster and crystal calculations are given elsewhere [13,14]. Here, we only give the salient features of our results.

3.1. Cluster results

The possibility of Mn forming stable clusters around N, with the manifestation of giant magnetic moment in Mn_xN clusters, was first predicted by Rao and Jena [15]. This opens up the question as to whether a TM impurity such as Mn can indeed go to the Ga substitutional site and form a local bond with N in GaN, while retaining the tetrahedral configuration of the lattice. The recently observed ferromagnetic coupling in MBE grown (GaMn)N sample with 14% Mn ($T_c \approx 750$ K) [7] reiterates this claim. As a precursor to full-fledged band calculations, we have carried out SCF-LCAO-MO cluster calculations on $(GaN)_x$ and $(GaN)_xTM_2$ (TM = Mn and Cr) clusters. Considering all possible spin multiplicities $M = 2S + 1$, we have obtained the optimized ground state geometries of these clusters (Fig. 1), using

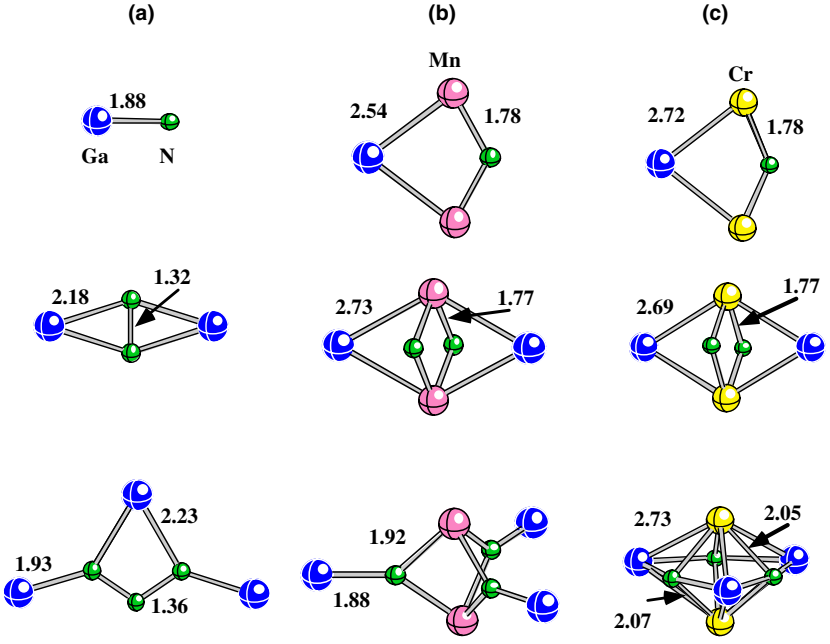

Fig. 1. Ground state cluster geometries for (a) $(GaN)_x$ (b) $(GaN)_xMn_2$ and (c) $(GaN)_xCr_2$ clusters ($x = 1$, 2, and 3).

Gaussian-98 code with LANL2DZ basis [16]. Our results are summarized in Tables 1–3. It is instructive to see first the results for dimers involving a cation and an anion or two cations (Table 1). For example, pure Mn_2 dimer is weakly bound, in sharp contrast to its neighbor Cr_2 which is very strongly bound. Mn–N has a higher binding energy and a smaller bond length compared to Ga–N, thereby indicating that Mn binds to N more strongly than Ga. Tables 2 and 3 summarize our calculated results for $(GaN)_x$ and $(GaN)_xTM_2$ clusters, respectively. The TM–TM distance in $(GaN)_xTM_2$ varies from ~3.1 Å (~3.3 Å) to ~2.4 Å (~2.7 Å) for TM = Mn (Cr), respectively. Guided by this, we carried out subsequently supercell band calculations with the Mn–Mn distance as 3.1 Å and Cr–Cr distance as 3.3 Å. The energy values quoted in Table 2 correspond to the following standard definitions viz:

(a) BE of $(GaN)_x$ clusters: $E_b = [xE(GaN) - E(GaN)_x]/x$,
(b) Energy gain in adding a GaN dimer to an existing $(GaN)_{x-1}$ cluster: $\Delta E_0 = E(GaN) + E[(GaN)_{x-1}] - E[(GaN)_x]$,
(c) Energy gain in adding a TM_2 dimer to an existing $(GaN)_x$ cluster: $\Delta E = E[(GaN)_x] + 2E(TM) - E[(GaN)_xTM_2]$.

The ΔE values for $x = 1$, 2, and 3 follow the same trend in the case of Mn and Cr-doping. The total magnetic moments of pure $(GaN)_x$ cluster for $x = 1$ turns out to be 2 μ_B (most of the moment being located at the N-site that is antiferromagnetically coupled to the moment at Ga site). With increasing cluster size, the

Table 1
Calculated ground state properties of dimers

Dimer	Bond length (Å)	Binding energy (eV)	Magnetic moment (μ_B)
Ga–N	1.88	2.18	2 [Ga: 0.31 N: 1.69]
Mn–N	1.60	3.07	4 [Mn: 4.09 N: −0.09]
Cr–N	1.59	2.06	3 [Cr: 3.51 N: −0.51]
Ga–Mn	2.60	1.36	4 [Mn: 4.66 Ga: −0.66]

Table 2
Energetics and magnetic moment of $(GaN)_x$ (see text for definitions)

x	E_b (eV)	ΔE_0 (eV)	Magnetic moment (μ_B)
1	0	–	2
2	2.99	4.02	0
3	3.33	3.66	0

Table 3
Energetics and magnetic moment of $(GaN)_x$ TM_2

	x	1	2	3
TM–TM dist (Å)	Mn:GaN	3.11	2.52	2.44
	Cr:GaN	3.29	2.62	2.74
TM–N dist (Å)	Mn:GaN	1.78	1.77	1.92
	Cr:GaN	1.78	1.77	2.05
Ga–N dist (Å)	Mn:GaN	2.88	2.73	1.88
	Cr:GaN	2.85	2.68	1.89
ΔE (eV)	Mn:GaN	5.39	3.73	4.34
	Cr:GaN	5.43	3.21	4.47
Multiplicity (μ_B)	Mn:GaN	8	4	8
	Cr:GaN	8	2	10

individual moments at Ga and N sites decrease and eventually vanish since bulk GaN is nonmagnetic. On doping with TM_2 the magnetic nature changes completely as seen from the optimized ground–state spin multiplicities $(M = 2S + 1)$ of $(GaN)_xTM_2$ clusters. For example, the total magnetic moment of $(GaN)_1Cr_2$ is 8 μ_B out of which 4.28 μ_B, 0.07 μ_B and -0.648 μ_B moments reside at Cr, Ga and N site, respectively. Bulk of the moments are localized at the TM site which are found to couple ferromagnetically, while the N sites acquire small moments and couple antiferromagnetically to those at TM sites. Thus, the ground states for both Mn_2 and Cr_2 doped $(GaN)_x$ are found to be ferromagnetic, with a lowering of energy by $\sim$0.4 eV.

3.2. Supercell band strucure

Bulk GaN crystallizes in wurtzite structure (space group $P6_3mc$) which has lattice vectors (in units of a) $(\sqrt{3}/2, -1/2, 0)$, $(0,1,0)$ and $(0,0,c/a)$ and an unit cell containing two cations at $(0,0,0)$ and $(2/3,1/3,1/2)$, and two anions at $(0,0,3/8)$ and $(2/3,1/3,7/8)$. There have been numerous first-principles investigations of the electronic properties of bulk GaN [17] as well as doped GaN [18]. In order to simulate TM_2 dimer doped GaN, we construct a 32 atom supercell with lattice vectors doubled along all the three directions, and then selectively replacing two Ga atoms with the impurity TM atom. Thus the supercell represents a $\sim$12% Mn-doped GaN DMS system and has formula unit $(TM_2Ga_{14})N_{16}$ whose cell parameters (see Table 4) have been taken from experimental data. TM–TM distance is fixed at nearest neighbor cation separation ($\approx$3.19 Å) which is more than the critical separation of 2.5 Å obtained from our cluster calculations reported in Section 3.1. Self-consistent spin-polarized TB-LMTO calculations [19] have been performed within the simplified atomic sphere approximation [20]. For details of the methodology followed, readers may refer to a recent review [21]. The atomic sphere radii ($s_{Ga} = 1.227$ Å, $s_N = 1.015$ Å), fixed by Hartree potential plot prescription, are found to be roughly proportional to the covalent radii ($r_{Ga} = 1.62$ Å, $r_N = 1.26$ Å). We have used $(6,6,4)$ k-mesh in all our supercell calculations, which corresponds to 144 k-points in the irreducible wedge of the Brillouin zone. Effect of structural relaxation

Table 4
$(Ga_{14}TM_2)N_{16}$ supercell: parameters and results

	$(Ga_{14}Mn_2)N_{16}$	$(Ga_{14}Cr_2)N_{16}$
Lattice parameters	$a = 3.189$ Å	$a = 3.189$Å
	$c = 5.185$ Å	$c = 5.191$Å
	$u = 0.377$	$u = 0.377$
TM d-band position	VB Top + 1.4 eV	VB Top + 1.6 eV
TM d-band width	2.4 eV	2.5 eV
Magnetic moment (μ_B)	Mn = 3.5	Cr = 2.69
	Ga = 0.02	Ga = 0.025
	N = −0.02	N = −0.025

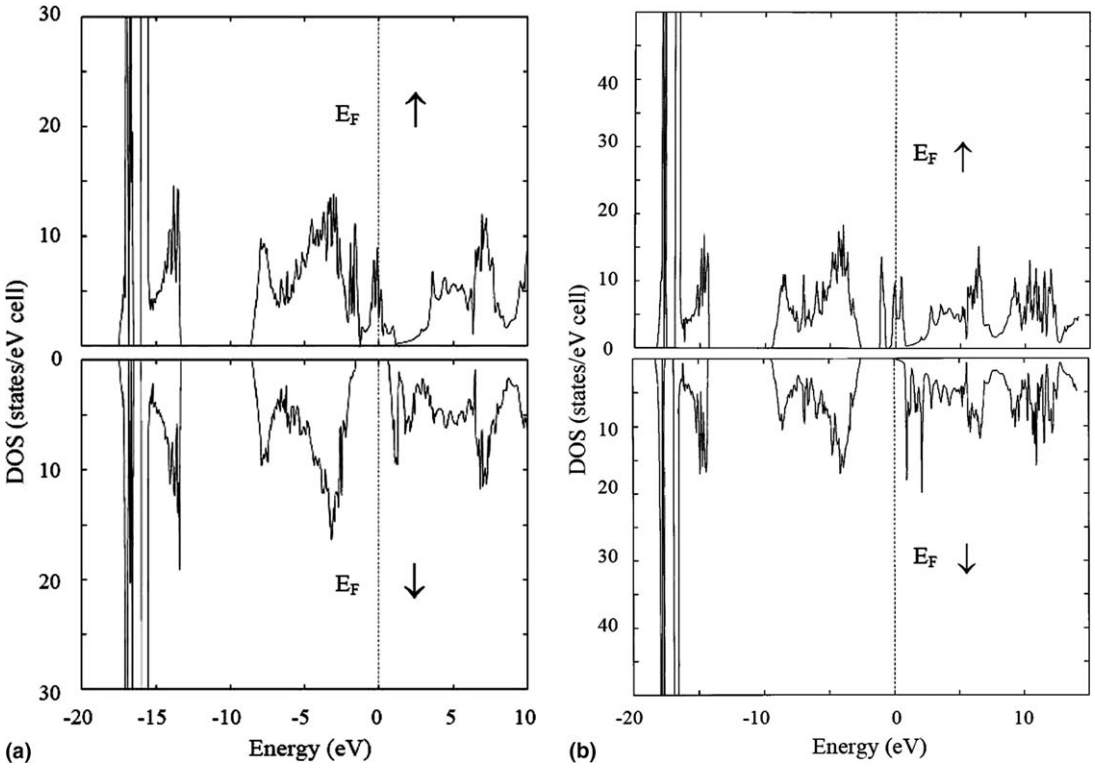

Fig. 2. Total DOS for majority-spin and minority-spin of (a) $(Ga_{14}Mn_2)N_{16}$ and (b) $(Ga_{14}Cr_2)N_{16}$ supercells.

has been neglected, since the replacement of a Ga atom of the semiconductor host by the impurity atom (Mn or Cr) is not expected to relax the lattice substantially [13,22].

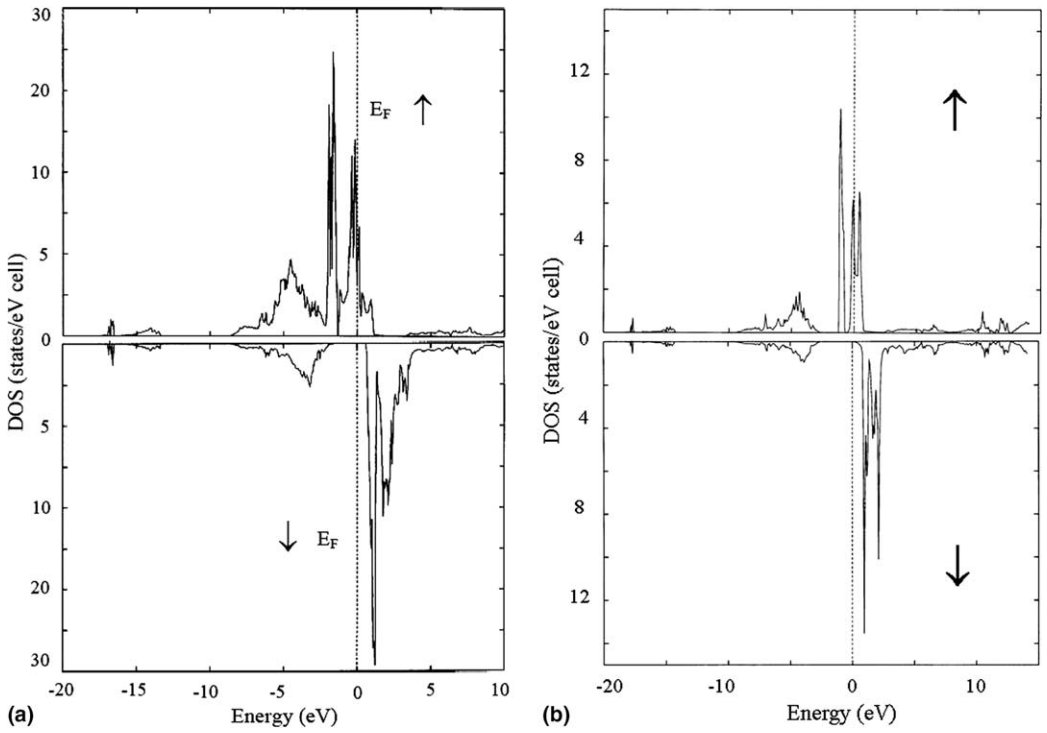

Fig. 3. Partial DOS projected on to the TM impurity site, for majority-spin and minority-spin of (a) $(Ga_{14}Mn_2)N_{16}$ and (b) $(Ga_{14}Cr_2)N_{16}$ supercells.

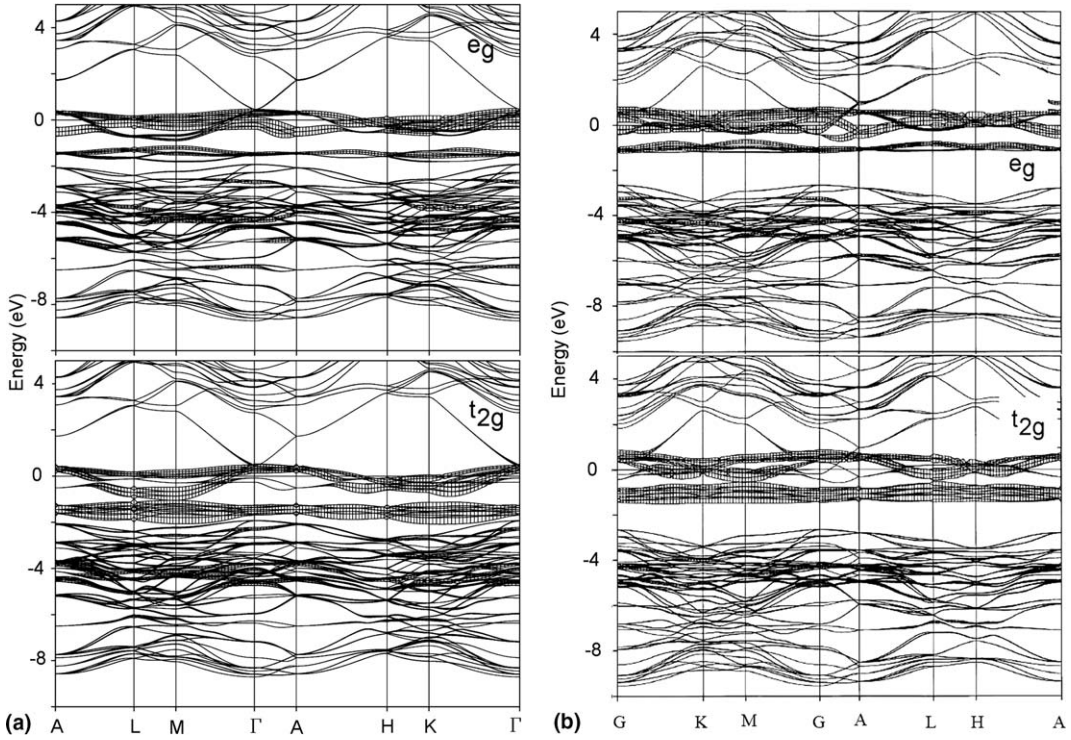

Fig. 4. Energy band structures of (a) $(Ga_{14}Mn_2)N_{16}$ and (b) $(Ga_{14}Cr_2)N_{16}$ supercells along high symmetry directions. Fermi level is at 0 of energy scale. The 'fat-bands' correspond to TM-e_g projected (top panel) and TM-t_{2g} projected (bottom panel). See text for details.

Self-consistent spin-polarized (only ferromagnetic) total densities of states of Mn- and Cr-doped GaN (Fig. 2) show the half-metallic behavior with 100% spin-polarization, that is ideal for injection of spin-polarized charge carriers into the non-magnetic semiconductor. Partial (TM-projected) DOS (Fig. 3) clearly shows that the states appearing in the gap are originating from the e_g and t_{2g} levels of the TM impurity, whose dispersions are seen from the so-called "fat-bands" projected onto the corresponding impurity d-orbitals (Fig. 4). Each of the fat bands has been allocated a width proportional to the (sum of the) weight(s) of the corresponding orthonormal orbital(s) [23]. The Mn-projected fat-bands show the minimum gap (direct) appearing at the M-point, while the Cr-projected fat-bands show the minimum gap at the Γ-point (Fig. 4). The Fermi level passes right through the fattened impurity band in both cases, indicating the possibility of double exchange mechanism to be the most likely mechanism for the ferromagnetic coupling in this family of DMS systems [24].

The paramagnetic DOS shows a ~2.4 eV wide Mn 3d-band hybridized with N 2p. The t_{2g} band lies above the e_g band, thereby indicating that the Mn is sitting in tetrahedral, rather than octahedral crystal field environment (i.e., if e_g. would have been above the t_{2g} band) in the GaN lattice. This is in conformity with the earlier results [10,11]. When spin-polarization is switched on, there is a further spin-splitting which we observe in the partial DOS as well as in the fat-bands. The peak of the majority-spin impurity d-band lies ~1.4 eV and 1.6 eV above the top of the valence band of GaN for Mn and Cr, respectively. This conforms to the accepted view that Mn is in d^4 configuration acting as an effective mass acceptor ($d^5 + h$), while Cr is in d^3 configuration. Deep-level optical spectroscopy measurements performed on lightly Mn-doped samples indeed show that Mn forms a deep acceptor level at 1.4 eV above the GaN band gap.

4. Conclusion and remarks

Ferromagnetism in Mn- and Cr-doped GaN has been investigated using first-principles density functional calculations within generalized gradient approximation. Density of states of $(Ga_{14}TM_2)N_{16}$ supercell show the Fermi level falling in the impurity band for majority-spin, while the minority-spin band merges with the conduction band bottom. Magnetic moments are found to be highly localized at the impurity sites with magnitudes ~ 3.5 μ_B for Mn and ~2.7 μ_B for Cr which are close to the corresponding cluster results (4 μ_B and 3 μ_B, respectively). Our cluster calculations reveal that in $(GaN)_x$ cluster, the coupling between the two TM's is ferromagnetic (total magnetic moment oscillating with x) while that between the TM and N is antiferromagnetic. This suggests that the ferromagnetic coupling between doped TM atoms is an indirect exchange mechanism mediated by N. These results are in agreement with the results earlier reported by van Schilfgaarde and Mrysaov [10]. Clustering of TM impurity atoms around N in GaN seems to play a crucial role in the manifestation of ferromagnetism in this class of dilute magnetic semiconductors. The sensitivity of the measured T_c's to experimental growth conditions may very well be due to the clustering of Mn around N that has been studied by several groups in the recent past [15,22,25].

Since clusters represent an extreme case of surface states and crystal sites represent a substitutional bulk environment, we conclude that doping of Mn in GaN whether they are porous, crystalline, or thin layers would lead to ferromagnetic coupling between Mn atoms. This allows great flexibility in synthesizing DMS systems involving Mn- and Cr-doped GaN. In fact, there are vigorous experimental efforts to realize DMS ferromagnetism in porous GaN that contains large internal surfaces and hence more substitutional sites. We are also now exploring the possibility of doping both Mn and Cr atoms together in the nearest neighbour and second nearest neighbour sites of host GaN lattice, and looking into the manifestation of DMS ferromagnetism.

References

[1] A.S. Wolf, D.D. Awschalom, R.A. Buhrman, J.M. Daughton, S. von Molnar, M.L. Rouckes, A.Y. Chtchelkanova, D.M. Treger, Science 294 (2001) 1488.
[2] M.N. Baibich, J.M. Broto, A. Fert, F.N. Van Dau, F. Petroff, P. Eitenne, G. Creuzet, A. Friederich, J. Chazelas, Phys. Rev. Lett. 61 (1988) 2472.
[3] G.A. Prinz, Science 282 (1998) 160.
[4] H. Ohno, Science 281 (1998) 951.
[5] T. Dietl, H. Ohno, F. Matsukura, J. Cibert, D. Ferrand, Science 287 (2000) 1019;
H. Ohno, D. Chiba, F. Matsukura, T. Omlya, E. Abe, T. Dietl, Y. Ohno, K. Ohtani, Nature 408 (2000) 944;
T. Dietl, H. Ohno, MRS Bull. 28 (2003) 714.
[6] C. Liu, F. Yun, H. Morkoc, J. Mater. Sci.: Mater. Electron. (JMSMEL), to appear.
[7] S. Dhar, O. Brandt, A. Trampert, L. Daweritz, K.J. Friedland, K.H. Ploog, J. Keller, B. Beschoten, G. Guntherodt, Appl. Phys. Lett. 82 (2003) 2077, and references therein.
[8] S.E. Park, H.-J. Lee, Y.C. Cho, S.-Y. Jeong, C.R. Cho, S. Cho, Appl. Phys. Lett. 80 (2002) 4187.
[9] V.I. Litinov, V.K. Dugaev, Phys. Rev. Lett. 86 (2001) 5593.
[10] M. van Schilfgaarde, O.N. Mryasov, Phys. Rev. B 63 (2001) 233205.
[11] K. Sato, H. Katayama-Yoshida, Jpn. J. Appl. Phys. 40 (2001) L485.
[12] T. Dietl, Physica E 10 (2001) 120;
T. Dietl, Semocond. Sci. Technol. 17 (2002) 377;
K. Sato, H. Katayama-Yoshida, Semicond. Sci. Technol. 17 (2002) 367;
S. Sanvito, G. Theurich, N.A. Hill, J. Supercond.: Incorporating Novel Magnetism 15 (2002) 85;
P. Mahadevan, A. Zunger, Phys. Rev. B 69 (2004) 11521.
[13] G.P. Das, B.K. Rao, P. Jena, Phys. Rev. B 68 (2003) 35207.

[14] G.P. Das, B.K. Rao, P. Jena, Phys. Rev. B 69 (2004) 24421.
[15] B.K. Rao, P. Jena, Phys. Rev. Lett. 89 (2002) 185504.
[16] M.J. Frisch et al., GAUSSIAN 98, Revision A.7, Gaussian, Inc, Pittsburgh, PA, 1998.
[17] M. van Schilfgaarde, A. Sher, A.B. Chen, J. Cryst. Growth 178 (1997) 8.
[18] C.G. van de Walle, S. Limpijumnong, J. Neugebauer, Phys. Rev. B 63 (2001) 245205.
[19] O.K. Andersen, O. Jepsen, Phys. Rev. Lett. 53 (1984) 2571, We have used the latest version of the Stuttgart TB-LMTO-ASA program. (Available from<www.mpi-stuttgart.mpg.de/Andersen>).
[20] O.K. Andersen, Phys. Rev. B 12 (1975) 3060.
[21] G.P. Das, Introduction to linear band structure methods, in: A. Mookerjee, D.D. Sarma (Eds.), Electronic Structure of Alloys Surfaces and Clusters, Taylor and Francis, London and New York, 2002, pp. 22–70.
[22] L.M. Sandratskii, P. Bruno, S. Mirbt, Phys. Rev. B 71 (2005) 04521.
[23] O. Jepsen, O.K. Andersen, Z. Phys. B: Condens. Matter 97 (1995) 35.
[24] K. Sato, P.H. Dedetichs, H. Katayama-Yoshida, J. Kudrnovsky, J. Phys.: Condens. Matter 16 (2004) S5491.
[25] Z.S. Popovic, S. Satpathy, W.C. Mitchel, Phys. Rev. B 70 (2004) 161308 (R).